TGFs and search for TGFs in AGILE, FERMI and RHESSI data by correlation with ground-based lightning measurements

Written by

Andreas Ramsli

Supervisors:
Ass. Professor, Martino Marisaldi
PhD cand., Anders Lindanger

Institute of Physics and Technology
University of Bergen
Norway

December 1, 2020

Contents

1 Introduction

Terrestial Gamma-ray Flashes (TGFs) are are millisecond long, very intense bursts of gamma-rays that can be associated to lightning and thunderstorm activity. The TGFs are observable manifestations of lightning activity, and they are produced in the most energetic natural particle accelerator on Earth (Dwyer,). Typical characteristics of a TGF is a duration around $100\mu s$, average fluence is $\approx 0.1cm^{-2}$ at satellite altitude (500-600 km) (Marisaldi et al.,), and this analysis finds that some TGF events can be associated to lightning activity with an association of $\pm 500\mu s$. Typically, these TGFs are observed from space. This analysis will use data from three spacecrafts; AGILE, Fermi and RHESSI, and data from the World Wide Lightning Location Network (WWLLN). The production models for TGFs are not completely understood, but a good understanding have been established. The basic physical mechanism responsible for TGF production is commonly believed to be the Relativistic Runaway Electron Avalanche (RREA) process (Marisaldi et al.,), which allows a seed electron of sufficiently high energy in a thundercloud electric field to overcome the friction force and increase it's energy up to relativistic values, and possibly produce secondary electrons that can drive an avalanche multiplication. Successive collision of relativistic electrons with air molecules lead to gamma-ray production by Bremsstrahlung. Although this model is widely accepted, there are several points still needing to be further explored, namely: the highest achievable energies, which translates into the maximum voltage drop that can be established within thunderclouds and the association to lightning.

1. Goal of the project is to understand how the same population of TGFs is detected in different ways by different spacecrafts
2. The student should determine the distribution of TGFs detected by AGILE, RHESSI and Fermi in longitude, latitude, local hour, counts and duration.
3. The student should find the closest WWLLN match to each AGILE and Fermi TGF, taking into account light travel time from source to the satellite, then he/she should find the list of AGILE and Fermi TGFs with a WWLLN association closer than $\pm 500\mu s$

Mission profile for the spacecraft is illustrated in the figure below. Note that the relevant orbits are illustrated in red, blue and green.

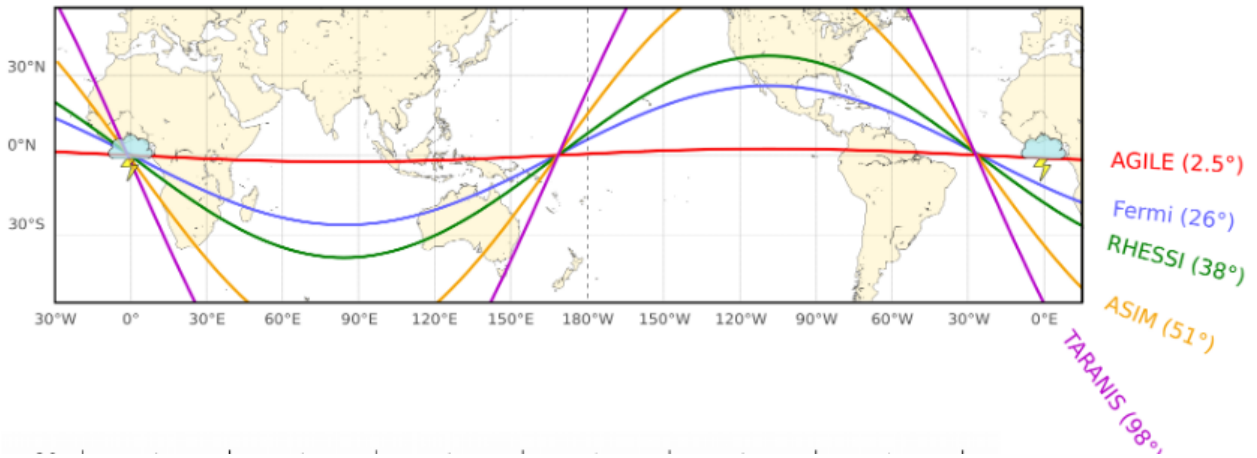

Figure 1: Graphical illustration of the orbital inclination for different spacecraft. AGILE, RHESSI and Fermi is relevant in this analysis.

2 Instruments and Datasets

2.1 Instruments

We have three satellites, each of them is capable of detecting high energy radiation. Actually, they are special because they are among the few satellites that can detect TGFs. Even though they all can detect TGFs, they do so in different ways with different instruments. To get a better understanding of how each spacecraft differ from each other, figure 2 gives a quick overview. This table is taken from (Lindanger,).

	RHESSI	AGILE MCAL	Fermi GBM
Operative	2002 -	2007 -	2008 -
Orbit altitude and inclination	38° 600 km	2.5° 540 km	26° 540 km
Detector type	HPGe	CsI(Tl) scintillator with solid state readout	NaI and BGO scintillator with PMT
Energy range	0.003 - 20 MeV	0.35 - 100 MeV	0.015 - 40 MeV
Effective area for typical TGF energy spectrum	260 cm^2	220 cm^2	160 cm^2 (1xBGO)
Acquisition type	continuous	triggered	triggered/continuous
TGFs/year	$\sim$ 340	$\sim$ 800	$\sim$ 800

Figure 2: Figure showing specs for the different satellites. Keep in mind that Fermi have two BGO detectors on board.

We will not go into too much detail on the instruments, but a quick overview can be helpful. Let's start with the Mini-Calorimeter (MCAL) on AGILE. Actually, the MCAL is a gamma-ray detector designed to detect cosmic gamma-ray bursts. With some adjustments, as I will explain shortly, the instrument could be used to detect gamma-rays from earth. Now, back to the MCAL. It consists of 30 CsI(Tl) scintillator bars, with a PIN photodiode placed at the end of each bar. A scintillator is an instrument that convert high energy radiation, such as X-rays or Gamma-rays, to near visible or visible light. Then the PIN-diode converts the light to an electronic signal. The intensity of the scintillation light is a function of the position of interaction along the bar, and the energy of the incoming particle (Lindanger,). The adjustments that was mentioned earlier was regarding the the anti-coincidence (AC) system. The aim of this system was to reject charged particles coming from the background. On 23. March 2015 the AC-system was turned off to enhance the detection of TGFs (Marisaldi et al.,). The motivation for such a change was the understanding that the dead time induced by the AC-system prevented the detection of a large fraction of TGFs. This resulted in enhancing the sensitivity for events lasting less than 100 μs. A vital aspect of the MCAL is that each of the scintillator bars works independently from each other, and each bar having a dead time of 20μs. Meaning, it takes 20μs for the system to be ready to take another measurement. We will now have a quick look at how AGILE records data.

In 2015 a software modification was implemented, resulting in an increase of one order of magnitude in TGF detection rate and enabling AGILE to detect TGFs with a shorter duration (Marisaldi et al.,). The mode used in this analysis is the BURST mode. In BURST mode each bar acts an independent detector. BURST mode is triggered, meaning the data is not a continuously recorded. The trigger logic acts on time windows from 293 μs to 8 ms (Marisaldi et al.,). For TGF search, the relevant time windows are 293 μs, 1 ms, and 16 ms. The static thresholds,i.e. the minimum of counts needed to issue a trigger, are 8, 10 and 41 counts, respectively (Marisaldi et al.,). After a trigger, data $\pm$1 sec, with respect to the trigger time, is sent to telemetry. The only parameters used

in this analysis, are the time of arrival and the location of the spacecraft.

On board Fermi there are several different types of instruments for detecting TGFs, but in this analysis we will focus on the two bismuth germanate (BGO) detectors. BGO is a crystal and works as a scintillator. To convert the photons emitted by the BGO to an electrical signal, Fermi uses Photomultiplier Tubes (PMT) instead of solid state detectors. As we can see from figure 2, the BGO detector have a lower energy threshold than AGILE.

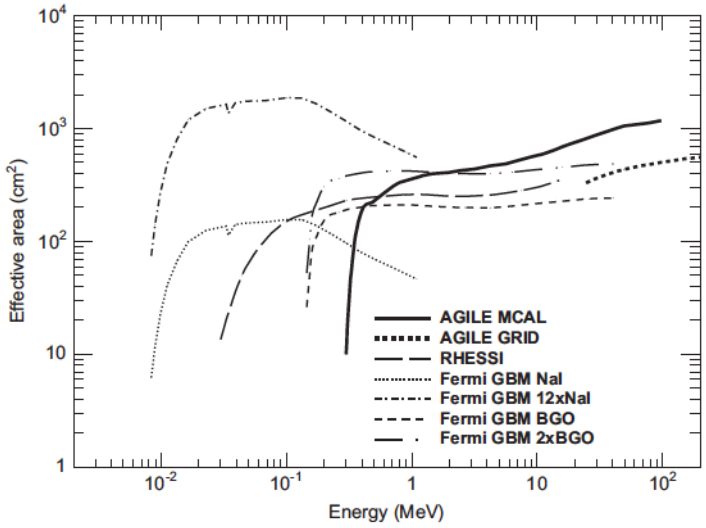

Figure 3: Energy range of the different detectors. Note that the scale is logarithmic

The 12 NaI(Tl) detectors measure the low-energy spectrum (8 keV to 1 MeV) and are used to determine the a coarse direction of cosmic gamma-ray bursts (GRBs), but cannot be used for the same purpose for TGFs because of the higher spectral hardness of TGFs. The counts from these detectors are in the Fermi catalog, but due to problems related to dead time with the NaI(Tl) detectors, these will not be included further in this analysis. Also, the BGOs have a higher energy range and large effective area for gamma rays. The use of the BGO detectors for triggering improved the average TGF detection rate from one per 32.5 days to one per 4.0 days, compared to the NaI(Tl) detector (Briggs et al.,).

The acquisition type for Fermi is triggered/continuous as we can see in the figure 2. To produce a triggered event the minimum online triggering interval is 16 ms, a hardware limit that cannot be improved upon. This resulted in a population of TGFs that was biased towards bright events, as in order to trigger. To overcome this continuous acquisition began on 9. July 2010 over specified regions where high TGF activity was expected and downlinked for each full orbit (Briggs et al.,). The enhanced dataset allowed TGFs to be studied over a range of intensities, rather than just the brightest events. Subsequent off−line searches using the time−tagged event (TTE) data allowed for the study of TGFs over shorter timescales than possible in orbit, resulting in a much higher detection rate. Finally, we will have a quick introduction to the RHESSI spacecraft.

The RHESSI spacecraft was initially designed to monitor solar photons with energies up to 20 MeV. With some adjustments, the spacecraft could instead help monitor the high energy photons

coming from earth itself. To do this, RHESSI used nine cryogenically cooled coaxial germanium detectors. This stands out from the two other spacecrafts. Only RHESSI had a cooling system like this. RHESSI telemeters all of its data to ground, allowing for a post-observation search for TGFs (Grefenstette, Smith, Hazelton, & Lopez,).

2.2 Datasets

In the following section we will have a look at the different datasets from the spacecrafts. A table of key metrics from the data is provided in table 1. Here the period, entries, mean duration and counts is presented.

Datasets			
Parameters	AGILE	Fermi	RHESSI
Period	23-03-2015 - 28-09-2018*	08-07-2008 - 31-07-2016**	01-03-2002 - 30-11-2013
Entries	2902 , 177*	4135	3345
Mean duration	T50: 121μs, Full: 242μs	Full: 320 μs	T68: 177 μs Full: 354 μs
Mean counts	17.6	23.9	24.0

*Table 1: * The search algorithm uses only the period from 19-01-2018*
*** The search algorithm uses only the period from 04-01-2016*

This is not a complete description of the dataset. The parameters that is used in this analysis, in addition to duration and counts, is: longitude, latitude, altitude (not for RHESSI) and UTC time. The coordinates is for the position of the spacecraft when the data was recorded. In addition to these parameters, it's relevant to construct a new one that we call local time. To do this, the UTC time and longitude coordinate is used to calculate the local time of the TGF event. As we know, 1 degree change in longitude results in a 4 minutes change in time. Later in this paper, we will see how these parameters are distributed. Before we get there, it's relevant to mention that the AGILE and Fermi dataset is reduced to a limited period (described in table 1). This is necessary because the data from the World Wide Lightning Location Network (WWLLN) is provided in a limited time period for each AGILE and FERMI.

The WWLLN dataset is as the name implies, a global lightning detection network consisting of 70 ground based stations that detect radio waves (3 - 30 kHz) from lightning flashes (Hutchins, Holzworth, Virts, Wallace, & Heckman,). The WWLLN data that is used in this analysis is a collection of files that contain the time and location of lightning sferic. WWLLN data are provided to Birkeland Centre for Space Science through a subscription service.

Figure 4 shows the relative detection frequency for the WWLLN network. Note that the detection efficiency on the African continent is relatively low, compared to the Americas and the Maritime Continent. The aim of this analysis is to find a correlation between the detected TGF event on board a spacecraft and lightning activity. Therefore is the WWLLN dataset used. In the following section the method for finding this correlation is explained further, but note that the longitude, latitude and UTC time is the key parameters that is used from the dataset.

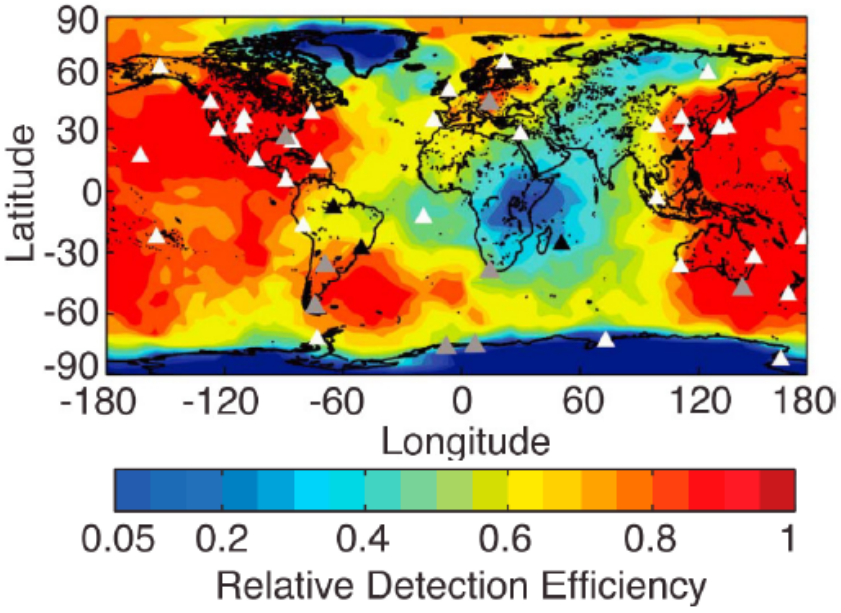

Figure 4: Relative detection frequency for the WWLLN network 16-6-2010. Operational stations are shown as white triangles, non operational as black, and partially active as gray. Figure from (Hutchins et al.,)

3 Methods

3.1 Managing of the datasets in preperation for plotting

Some minor changes to the dataset had to be done in preparation for plotting. For example, the longitude values that was rangeing from 0 to 360 was converted to range between ± 180. Local hour had to be calculated from the UTC time and the longitude position of the spacecraft. Note that 1° change in longitude, results in a 4 minute change. The algorithm for this can be found in the GitHub repository. Link to this is provided at the end of the paper.

3.2 Reduction of dataset size

This following section explains step by step how the datasets were reduced to fit the search algorithm. This algorithm is provided in the GitHub repository. The aim of this algorithm is to find AGILE and Fermi TGFs with a WWLLN association closer than $\pm 500 \mu s$.

1. The first step was to filter out the entries in the AGILE and Fermi that can't be associated to a WWLLN file. The algorithm searches through the WWLLN files in the time period that is specified in table 1.
2. Next step in the algorithm is to access the correct WWLLN file. The algorithm will access a file that has the same timestamp as the recorded event on board the spacecraft. UTC time is used in all datasets.
3. When searching for a WWLLN association, the algorithm filters out lightning locations that is further than 1000 km from the spacecraft. Constraining the search to a maximum distance of 1000 km on the surface of earth between the satellite and lightning. The selected 1000 km radius is based on (Connaughton et al.,). Cummer et al., found most WWLLN matches

within 300km from the sub-satellite point (Cummer et al.,). Only Cohen et al., found some matches up to 1000 km (Cohen, Inan, Said, & Gjestland,). Figure 6 illustrates the TGF field of view.

4. Once a match had been found through the search algorithm, they were benchmarked against the AGILE catalog manually.
5. It is also taken into account that WWLLN sometimes detects the same lightning flash several times. Two WWLLN detections, close enough in time and location to be associated with the same counts detected by AGILE, would result in a detection of two TGFs instead of one. Therefore, if two lightning flashes are closer in time and location than one time bin (100 μs) in the analysis, only one is kept. This is done by taking the difference of (time-lightning + time-propagation time) for lightning 1 and lightning 2.

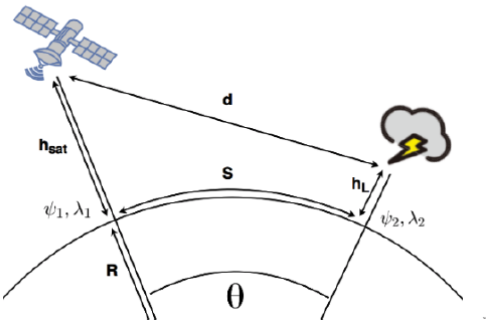

Figure 5: Satellite. Figure from (Lindanger,)

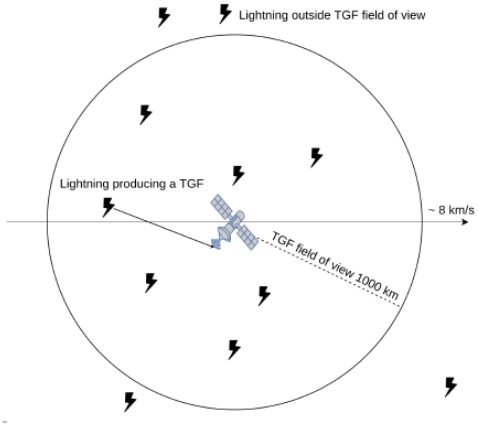

Figure 6: Lightning radius. Figure from (Lindanger,)

3.3 Propagation time of photons associated to TGF

To find a WWLLN association three parameters need to be calculated. First, the great circle distance, S, is given by the haversine function in (1). The parameters used in (1) is illustrated in figure 5.

$$S = 2R \arcsin \sqrt{\sin^2\left(\frac{\psi_2 - \psi_1}{2}\right) + \cos\left(\psi_1\right)\cos\left(\psi_2\right)\sin^2\left(\frac{\lambda_2 - \lambda_1}{2}\right)} \tag{1}$$

Once S is calculated, the angle θ can be obtained by the following relation: $\theta = \frac{S}{R}$, where R is the average equatorial radius of the earth. Also, the h_L parameter, which is the height of the source altitude, is set to be 15 km, as (Lindanger,) suggest. This angle is used in the law of cosines function (2). Equation (2) calculates the distance the photons travels distance photons travel from the TGF to satellite. Figure 5 illustrates the different parameters used in (2).

$$d^2 = (R + h_{sat})^2 + (R + h_L)^2 - 2(R + h_{sat})(R + h_L)\cos\left(\theta\right) \tag{2}$$

To find a association, the recorded time of TGF event needs to be corrected by the propagation time of the photon. Once the time has been corrected, a correlation can be found if the difference between the corrected TGF event and WWLLN time is within $\pm 500 \mu s$.

4 Results

In the two following sections the various results will be presented. First, the distribution of TGFs from AGILE, Fermi and RHESSI. Second, the results from the AGILE catalog that have a WWLLN association, as explained in section 3.2

4.1 Distribution of TGFs

In figure 7 the distribution of TGFs detected by AGILE, RHESSI and Fermi is presented in four different histograms. The parameters are: longitude, latitude, local hour and number of counts. On the y-axis it shows how many counts that is recorded in each bin. Keep in mind that the bin size differ between the histograms (labeled under the x-axis). First, let's take a closer look at the longitude distribution.

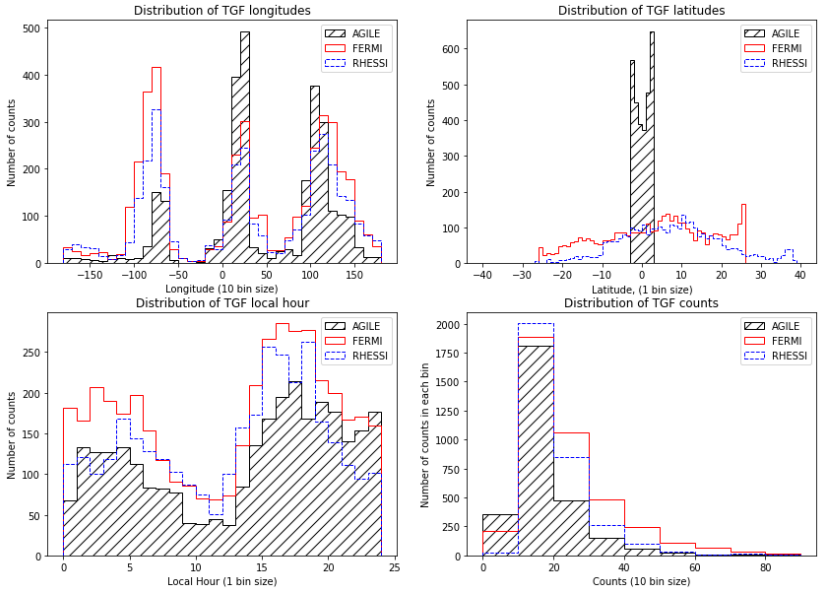

Figure 7: Distribution in longitude, latitude, local time and counts. Bin size are labeled under each X-axis

There is one common feature for all three spacecrafts; the distribution in longitudes clearly show three-continental lightning chimneys. The TGF active regions is defined as three-continental longitude bands: Central America: $[-90°, -60°]$; Africa: $[-10°, +30°]$; and Maritime Continent:$[+100°, +150°]$.

The latitude distribution is shown in the upper right histogram. What stands out in the latitude distribution is the horns produced by the data from AGILE. As we can see, they spike at $\pm 2,5°$, which is the orbital inclination of the spacecraft. On the other hand, Fermi and RHESSI is more distributed, but we do see a spike for Fermi at $+25°$. Their inclination is $\pm 25.6°$ and $\pm 38°$, respectively.

The plot in the bottom left shows the distribution of the local hour detected. We do see morning/afternoon peaks for all three spacecraft.

At the bottom right we find the distribution of counts. This histogram shows for instance that AGILE is able to detect the highest number of low counts in the fist bin, ranging from 0-10 counts. While RHESSI have a very low count in this bin, compared to the two others. This is in contrast to the next bin, ranging from 10-20 counts. In this bin, RHESSI have highest number of counts. One thing this distribution shows is that they have a relatively similar distribution. Meaning, it can be expected that that most of the counts fall in the range of 10-20 counts.

In figure 8 a plot of the geographical points is illustrated. The data that was used in this plot is from the Fermi catalog. The figure is taken from (Roberts et al.,).

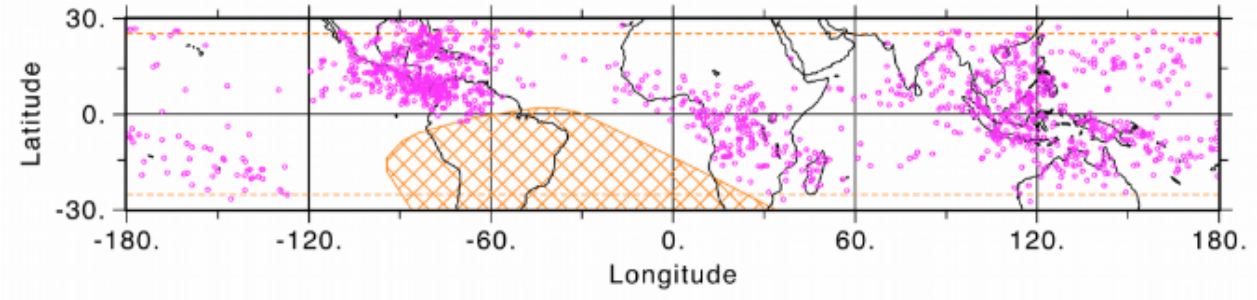

Figure 8: Geographical points of detection for TGFs in the Fermi catalog. The South Atlantic Anomaly (SAA) is the yellow hatched area.

Figure 9 is a histogram showing the the distribution of duration of a TGF event. Note that a logarithmic scale is used on x-axis. The bin width in this histogram was determined by the Freedman-Diaconis rule (Freedman & Diaconis,). Why we see the spikes in the Fermi data is discussed under "duration" in section 5.1

First of all, it's important to note that each spacecraft determines the duration different. This is shown in the legend. The AGILE T50 duration is determined by the time it takes for 50% of the counts to be recorded. On the other hand, RHESSI is determined by the time it takes for one σ (68%) of the counts to be recorded. Lastly, the Fermi duration is the the time of the whole event. From the plot we see that the duration of a TGF event (δt) is roughly $10\mu s < \delta t < 1ms$. That's three orders of magnitude difference. However, the way AGILE and RHESSI determines δt have shifted the plots to the left. AGILE the most since 50% of the counts are used. While this is the case, the expected value for duration is around $100\mu s$ for all three spacecrafts.

4.2 TGFs from AGILE with a WWLLN association

As mentioned in section 2 and 3, the AGILE dataset was reduced to a limited time period to fit the WWLLN dataset. This reduced the number of TGFs from 2902 to 177. Given this, the search algorithm found 106 TGFs that have a WWLLN association closer than $\pm 500\mu s$. At the present time, the search algorithm is designed to find a WWLLN association from the AGILE datasets. Some adjustments have to be made before the algorithm can search through the data from Fermi. Recently the website that provided the data for AGILE can't provide the WWLLN data associated to each TGF. Therefore it was not possible to update the dataset, and the comparison of counts

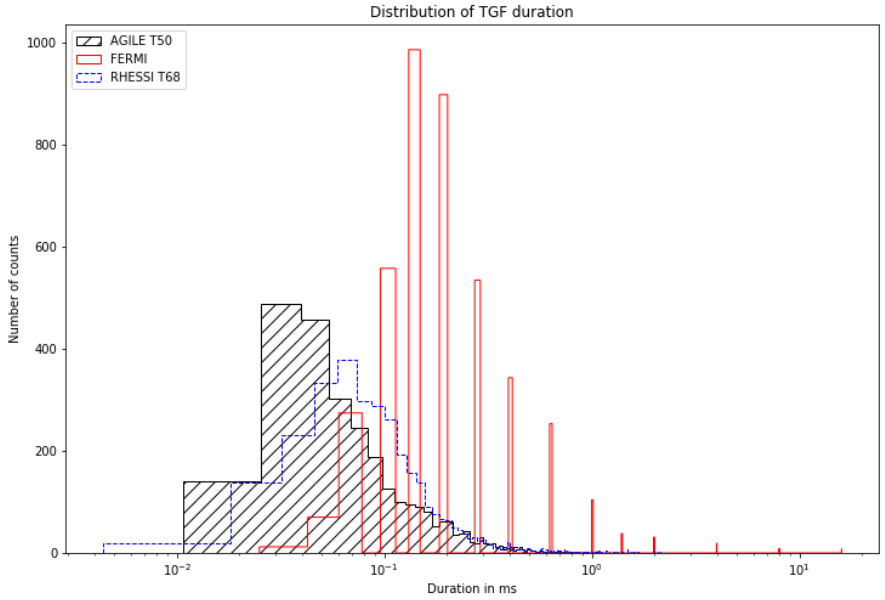

Figure 9: Figure showing distributions of the TGF duration. AGILE is hashed and marked black. Fermi is marked red. RHESSI is dotted and marked blue. Note that the x-scale is logarithmic.

and duration is left out. However, the the results from the current algorithm is presented in the following section.

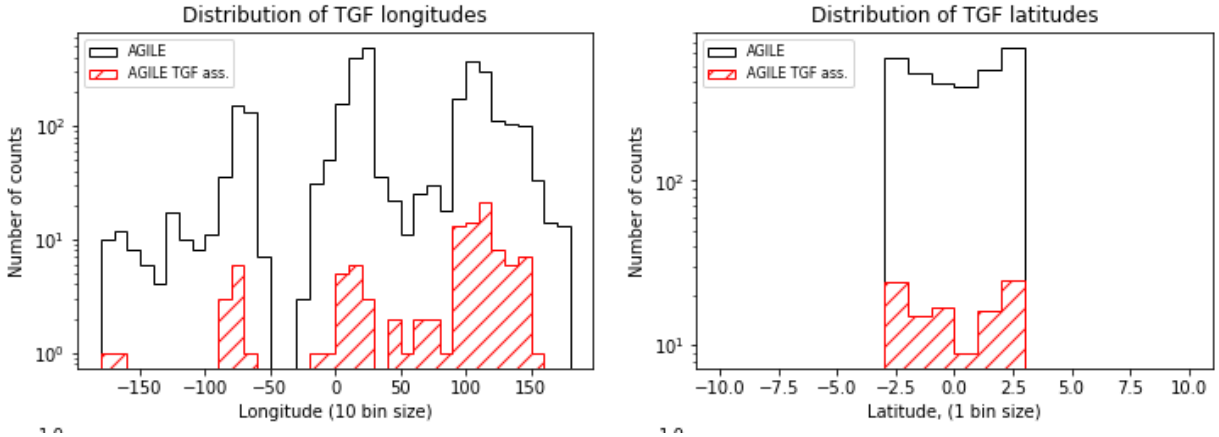

Figure 10: An updated histogram of the longitude and latitude distribution. TGFs from AGILE are plotted in black and the ones that have a WWLLN match are plotted hatched and red. Note that the y-axis has now a logarithmic scale, so that the TGFs with an association can be better shown.

To get a better understanding of where the TGFs is occuring, figure 11 shows the geographical locations. The longitudinal values for the lightning chimneys that was found in figure 7 is labeled along the X-axis. Note that the inclination of AGILE is $\pm 2.5°$.

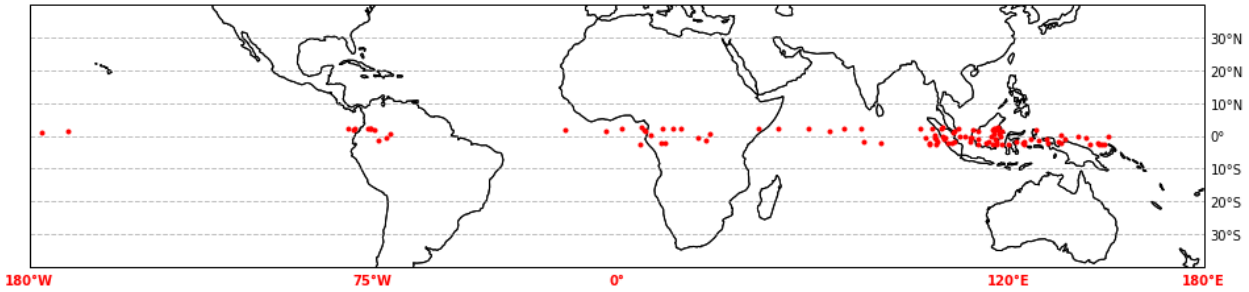

Figure 11: A scatter plot of the geographical location of the TGFs that have a WWLLN association closer than $\pm 500 \mu s$

5 Discussion

5.1 Distribution of TGFs

Longitude
As we can see, the geographical distribution is peaked in tropical regions. This indicates that thunderstorms influenced by the strong convective air currents (typical of those regions) can generate TGFs (Tavani et al.,). For AGILE, the highest concentration of TGFs seems to be found on the Maritime Continent, while the lowest concentration seems to be found in Central America. Meanwhile, Fermi and RHESSI have considerable higher number of counts in the Central America region. The reason for this might be because of the 2.5° inclination of the orbit. Since FERMI and RHESSI have a higher inclination, they will travel over the Caribbean, where there is more weather systems. Meanwhile, AGILE will pass over the mainland. Evidently, fewer TGFs is produced over mainland compared to large bay regions along the coastline, such as the Caribbean.

Latitude
AGILE and Fermi have very different orbits and observe different areas. Since the inclination of AGILE is so low, it allows the spacecraft to observe a narrow band around the equator. AGILE cannot observe Australia, where Fermi finds the highest TGF/lightning ratio (Briggs et al.,). On the other hand, the histrogram shows two horns in the latitude distribution for AGILE. The explanation for this because the spacecraft spends more time at the edges of the inclination rather at the equator. Despite the different areas observed, the geographic ratios found by the two instruments could be considered similar for Fermi and RHESSI.

As the latitude distribution shows, there is a relatively low number of events at the lower latitudes for RHESSI and Fermi. This might be explained by the orbital inclination (illustrated in figure 1). Take RHESSI for instance. Even though the inclination extends to $-38°$, there is no significant number of events that extends beyond $-10°$ (Keep in mind that the northernmost point of Australia is at around $-10°$). On the other hand, there is a relatively high number of events beyond $+10°$. The reason for this might be because we find more areas that contains weather systems that produce lightning activity. Examples are Central America and the Maritime Continent. Another explanation is that the South Atlantic Anomaly (SAA), is at it's strongest at between the latitudes $-15°$ to $-30°$ (Heirtzler,). Because of the weak magnetic field in this region, high energetic particles are able to penetrate further into the the atmosphere, possibly damaging the spacecraft. To prevent this, the spacecrafts have mechanisms to protects it's instruments from damage. For instance, the GBM on board Fermi is off while passing through the SAA. On the other hand, while

searching for the same mechanism for RHESSI, the papers didn't mention anything about this, but there is reason to believe the spacecraft have a similar mechanism. On the other hand, because of the background noise in SAA, it would be very hard to detect a TGF in this region. In summary, there is a higher number of TGFs in the lower latitudes than the higher. One reason that might explain this, is be because of geographical areas in the lower latitudes, such as Central America and the Maritime Continent. These regions have more frequent and strong weather systems. It is also important to keep in mind that the SAA above South America and the protective mechanisms on board affect the number of TGFs found in this region.

Local hour
The peaks that is shown in the local hour distribution shows early morning/afternoon peaks. These times are typically when storm systems are the most active. In the histogram, we do see that Fermi have the highest number of events. This is because the dataset is larger than the two other. On the other hand, the central trend is the same for all three spacecrafts; early morning/afternoon peaks.

Counts
As mentioned in the previous section, AGILE have the highest number of events in the first bin. There might be several reasons for this. First of all, the errors in all of these plots have not been taken into account. On the other hand, the difference is almost 300 events, so one might suspect that difference is caused by the instruments.

As it was presented in table 1, the mean value for counts is 17.6, 23.9, 24.0 for AGILE, Fermi and RHESSI, respectively. The distribution of TGF intensity follows approximately a power law, meaning that low intensity are much more common than high intensities. For that reason, it could be expected that the highest number of counts would be found in the bin ranging from 10-20, as we see in figure 7.

Duration
The spaced out spikes that we see in the Fermi plot is because of the binning of the data in the Fermi catalog. The binning approach that is used are bin widths from $25\mu s$ to $16ms$. These bins is provided in table 2 in (Briggs et al.,) and they match the location of the spikes that we see in figure 9. As mentioned in the previous section, the spacecrafts uses different methods for defining a TGF duration. Depending on how one views the plot, the histograms have been shifted, but they follow the same trend. The expected value for a TGF duration lies around the $100\mu s$. To elaborate a little further on the AGILE distribution, the MCAL instrument on board AGILE (see section 2) might be able to detect a higher number of short duration TGFs because they work in parallel, and is not affected by dead time of the other scintillator bars. In BURST mode each bar acts an independent detector with an average dead time of $20\mu s$. As we can see in figure 9, AGILE detects more TGFs below the $100\mu s$ range. On the other hand, the Fermi spacecraft uses different instrumentation for detection of TGFs, resulting in a different distribution.

Summary
Some of the key findings in this analysis is that TGF occurrence depends on location, local weather conditions and local time. Instruments do also have an effect on TGF detection. Each spacecraft

has it's own advantages and limitations. As a little side note, it would be interesting to correlate energy and duration. This is not done in this analysis, but it would be interesting to do.

5.2 TGFs from AGILE data with a WWLLN association

The search algorithm found 106 TGFs with an association closer than $\pm 500 \mu s$ from the WWLLN dataset. The number of TGFs in the given time period (given in 1) was 177. That is a association rate of around 60% . Given the relative detection efficiency by WWLLN, this is a decent number.

As we saw in figure 11, most of the TGFs that have a lightning association is located on the Maritime Continent. There might be several factors for why the concentration is much higher in this area, compared to the other two TGF chimneys found in figure 7. The relative lightning detection efficiency, as can be seen in figure 4, indicate that the Maritime Continent have a detection efficiency above 0.8 around the 120° longitudinal region. This is in contrast to the the efficiency on the Central American – and especially on the African continent. On the latter, the efficiency is between 0.2 and 0.4. Then again, the lightning chimney in the African region, given in figure 7, indicate that there is substantial TGF detection.

Considering the number of TGFs detected by AGILE in this region and the number of TGFs that have a WWLLN association, it can be concluded that the correlation is affected by the the relative detection efficiency by WWLLN in this region. The number of TGFs with an association might be much higher had the efficiency of WWLLN in this region been better.

In the Central American region the relative detection efficiency is higher than the African region (about 0.6). Despite this, the number of TGFs that have an association in this Central America is actually less than the number found in Africa. On the other hand, AGILE detected a relatively low number of TGFs in Central America. The reason for this was discussed in the previous paragraph on the longitudinal distribution.

6 References

The search algorithm, python script and CSV file of the AGILE TGFs (WWLLN ass.) with the propagation time parameter can be found on Github:

https://github.com/AndreasRamsli/TGF

Datasets
AGILE: https://www.ssdc.asi.it/mcal3tgfcat/
Fermi: https://fermi.gsfc.nasa.gov/ssc/data/access/gbm/tgf/
RHESSI: http://scipp.pbsci.ucsc.edu/rhessi/

References

Briggs, M. S., Xiong, S., Connaughton, V., Tierney, D., Fitzpatrick, G., Foley, S., ... others (2013). Terrestrial gamma-ray flashes in the fermi era: Improved observations and analysis methods. *Journal of Geophysical Research: Space Physics*, *118*(6), 3805–3830.

Cohen, M. B., Inan, U. S., Said, R. K., Gjestland, T. (2010). Geolocation of terrestrial gamma-ray flash source lightning. *Geophysical Research Letters*, *37*(2).

Connaughton, V., Briggs, M., Holzworth, R., Hutchins, M., Fishman, G., Wilson-Hodge, C., ... others (2010). Associations between fermi gamma-ray burst monitor terrestrial gamma ray flashes and sferics from the world wide lightning location network. *Journal of Geophysical Research: Space Physics*, *115*(A12).

Cummer, S. A., Zhai, Y., Hu, W., Smith, D. M., Lopez, L. I., Stanley, M. A. (2005). Measurements and implications of the relationship between lightning and terrestrial gamma ray flashes. *Geophysical Research Letters*, *32*(8).

Dwyer, J. R. (2012). The relativistic feedback discharge model of terrestrial gamma ray flashes. *Journal of Geophysical Research: Space Physics*, *117*(A2).

Freedman, D., Diaconis, P. (1981). On the histogram as a density estimator: L 2 theory. *Zeitschrift für Wahrscheinlichkeitstheorie und verwandte Gebiete*, *57*(4), 453–476.

Grefenstette, B., Smith, D., Hazelton, B., Lopez, L. (2009). First rhessi terrestrial gamma ray flash catalog. *Journal of Geophysical Research: Space Physics*, *114*(A2).

Heirtzler, J. R. (2002). The future of the south atlantic anomaly and implications for radiation damage in space. *Journal of Atmospheric and Solar-Terrestrial Physics*, *64*(16), 1701–1708.

Hutchins, M., Holzworth, R., Brundell, J., Rodger, C. (2012). Relative detection efficiency of the world wide lightning location network. *Radio Science*, *47*(06), 1–9.

Hutchins, M., Holzworth, R., Virts, K., Wallace, J., Heckman, S. (2013). Radiated vlf energy differences of land and oceanic lightning. *Geophysical Research Letters*, *40*(10), 2390–2394.

Lindanger, A. (2018). *Search for terrestrial gamma-ray flashes in agile data by correlation with ground-based lightning measurements* (Unpublished master's thesis). The University of Bergen.

Marisaldi, M., Argan, A., Ursi, A., Gjesteland, T., Fuschino, F., Labanti, C., ... others (2015). Enhanced detection of terrestrial gamma-ray flashes by agile. *Geophysical research letters*, *42*(21), 9481–9487.

Marisaldi, M., Fuschino, F., Labanti, C., Tavani, M., Argan, A., Del Monte, E., ... others (2013). Terrestrial gamma-ray flashes. *Nuclear instruments and methods in physics research section A: Accelerators, spectrometers, detectors and associated equipment*, *720*, 83–87.

Marisaldi, M., Fuschino, F., Tavani, M., Dietrich, S., Price, C., Galli, M., ... others (2014). Properties of terrestrial gamma ray flashes detected by agile mcal below 30 mev. *Journal of Geophysical Research: Space Physics*, *119*(2), 1337–1355.

Roberts, O., Fitzpatrick, G., Stanbro, M., McBreen, S., Briggs, M., Holzworth, R., ... Mailyan, B. (2018). The first fermi-gbm terrestrial gamma ray flash catalog. *Journal of Geophysical Research: Space Physics*, *123*(5), 4381–4401.

Tavani, M., Marisaldi, M., Labanti, C., Fuschino, F., Argan, A., Trois, A., ... others (2011). Terrestrial gamma-ray flashes as powerful particle accelerators. *Physical review letters*, *106*(1), 018501.